JOURNAL OF MATERIALS SCIENCE 31 (1996) 5593–5601

The effect of glass bead content on the mechanical properties of acrylonitrile/styrene/acrylate copolymer

Z.U. NABI, S. HASHEMI
School of Polymer Technology, University of North London, Holloway Road, London N7 8DB UK

The influence of glass bead content and the loading rate on the mechanical properties of polyacrylonitrile/styrene acrylate (ASA) copolymer was investigated. For this copolymer, tensile yield strength and work to fracture were significantly reduced as the bead content was increased. Tensile yield strength decreased linearly with increasing glass bead content according to the Leinder equation. It was found that the variation of tensile yield strength with log(loading rate) follows that of Eyring's equation for yielding. The presence of the weldline reduced the tensile yield strength of both unfilled and filled materials. Flexural modulus and flexural strength also varied in a predictable fashion with glass bead concentration. The increase in modulus with glass bead content followed Kerner's equation.

Crack growth resistance values of the unfilled ASA and its composites were measured at three loading rates using the generalized locus method. It was found that the resistance to steady crack propagation, J_R, was a sensitive function of glass bead content and loading rate. Within the range of these experiments, J_R decreased with increasing glass bead content and loading rate.

1. Introduction

Solid glass spheres are commonly added to thermoplastics as a reinforcing filler. In plastic applications, the spherical shape allows the glass spheres to act as tiny ball bearings and thereby increase the flow rate of the polymer. The sphericity of the glass beads also yields better stress distribution. This is important since stress within moulded sections often leads to premature failure. The isotropic behaviour of spheres provides uniform shrinkage which is an important factor in their use in plastics. However, while unique properties, such as dimensional stability or increased modulus are the usual motivation for exploiting glass bead-filled composites, special attention must be paid to other mechanical properties such as tensile yield strength and fracture toughness. In addition one also needs to consider the influence of weldline on tensile properties, as almost all glass filled materials are primarily injection moulded. Weldlines that are formed by the merging or impingement of separate melt flow fronts are often a potential source of mechanical weakness and therefore if present, can influence the load-bearing capability of the moulded parts.

The material chosen for this research study is acrylonitrile–styrene–acrylate (ASA) copolymer filled with six levels of glass bead content ranging from 1.5 to 18.5% by volume. Deformation behaviour of the unfilled ASA and its composites was studied through a series of tensile and flexural tests on unnotched specimens. Fracture studies involved testing single edge notched bend specimens in three-point bend configuration. Since unfilled ASA and its composites were consistently failed in a ductile manner, the resistance to crack propagation, J_R, was considered to be of primary importance. Crack growth resistance values were measured as a function of glass bead content using the generalized locus method. Moreover, since the influence of loading rate on material performance is an important consideration in material selection, deformation and fracture studies were performed by varying the loading rate between 5 and 500 mm min^{-1}.

2. Material description

Acrylonitrile–styrene–acrylate (ASA) polymer under the tradename Luran S was selected as the matrix for this study. This material is made by the copolymerization of styrene and acrylonitrile (SAN) in combination with a grafted acrylic ester elastomer. The elastomer is in the form of very finely divided particles uniformly distributed in the SAN frame work and bonded to it by grafted SAN chains. Spherical CPO3 glass beads coated with silane coupling agent of type 3000 were used as a filler material. The particle mean diameter was in the range 12–26 μm.

0022–2461

3. Preparation of the composite materials and the test specimens

Six composites containing different amounts of glass bead were prepared in-house. Composites were prepared by first mixing preweighed quantities of ASA pellets and glass beads manually followed by compounding in a twin screw extruder (Leiteritz) fitted with a 2 mm rod die. The melt temperature was kept constant at 270 °C and the screw speed was 200 r.p.m. The extrudates were then granulated for injection moulding of test pieces.

After compounding, each of the composites and the unfilled resin were injection moulded into tensile and flexural bars as shown in Fig. 1. The materials were dried in an oven prior to moulding as per manufacturer's recommendations. All the specimens were moulded after the machine had attained steady state with respect to the preset melt and mould temperatures.

The mould used to prepare tensile specimens consisted of two dumbbell-shaped cavities each 1.7 mm thick as shown in Fig. 1(a). One of these was filled with the molten material entering the mould from one end and the other was filled with molten material entering from both ends. In the latter case a weldline was formed at the centre of the moulding as a result of two impinging flow fronts.

Flexural specimens were moulded using an edge-gated rectangular cavity of dimensions $120 \times 10 \times 4$ mm as shown in Fig. 1(b).

To fabricate these test pieces, the processing conditions had to be altered slightly in order to produce complete mouldings. The range of conditions employed to produce test specimens are given in Table I.

To determine the exact weight fraction of the glass beads in the test specimens, several tensile and flexural bars were randomly selected for the ash test. The weight fraction, w_f, of the glass bead for all six composites was then determined from which the volume fraction, ϕ_f, was calculated from the following equation;

$$\phi_f = \left[1 + \frac{\rho_f}{\rho_m}\left(\frac{1}{w_f} - 1\right)\right]^{-1} \quad (1)$$

where ρ_m is the density of the matrix (1.07 g cm^{-3}) and ρ_f is the density of the glass bead (2.54 g cm^{-3}).

TABLE I Moulding conditions

Melt temperature	270 °C
Mould temperature	70 °C
Injection pressure	50–100 × 10^5 Pa
Cooling time	20 s

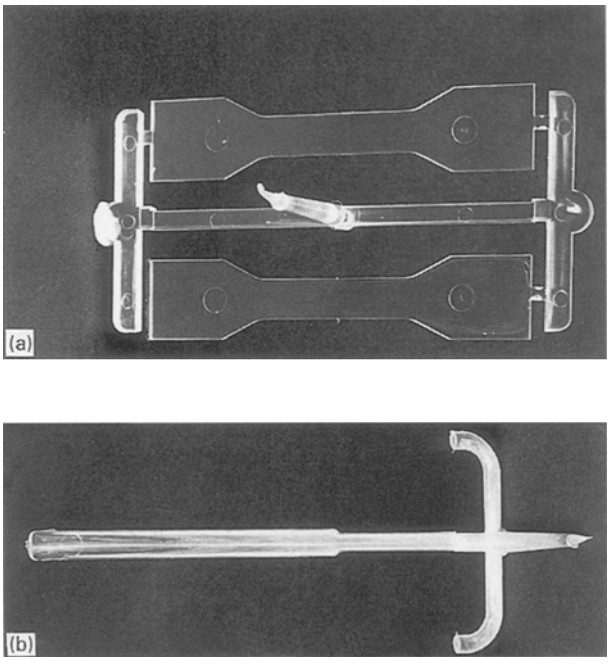

Figure 1 (a) Dumbbell specimens, (b) flexural bar.

4. Results and discussion

4.1. Tensile tests

Tensile tests were carried out on the dumbbell shaped specimens with and without weldlines in an Instron testing machine at room temperature and at crosshead displacement rates between 2 and 200 mm min^{-1}. The samples for the tensile tests were 1.5 mm thick with a constant width of 12 mm along the gauge length of 50 mm. A minimum of four specimens were tested for each material at a given crosshead speed.

Fig. 2 shows some typical tensile load–displacement diagrams for ASA polymer and its composites. As can be seen, ASA polymer and its composites exhibit a clear yield point from which tensile yield strength, σ_y, (maximum load divided by the original cross-sectional area) was calculated. Other quantities measured where tensile strength at break, σ_b, and the total energy under the load–displacement diagram (work of fracture). All these quantities were plotted as a function of glass bead content, ϕ_f.

The effect of glass bead content on tensile yield strength is illustrated in Fig. 3 for crosshead speeds ranging from 2 to 200 mm min^{-1}. Plots show that

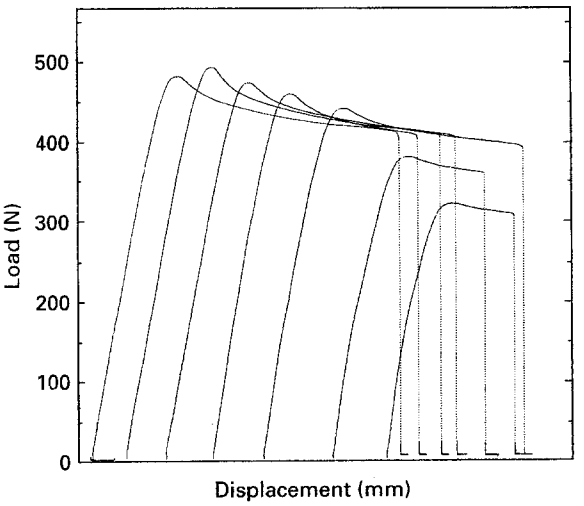

Figure 2 Typical tensile load–displacement diagrams for ASA polymer and its composites at loading rate of 5 mm min^{-1} (From left to right for: 0%, 2%, 3.5%, 5%, 7.2%, 12.2% and 18% by volume glass beads.)

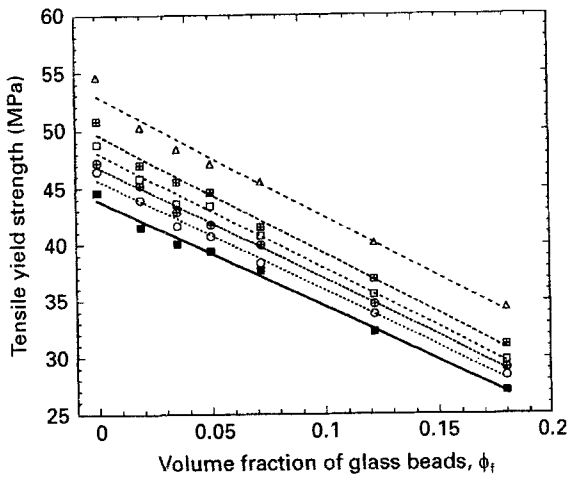

Figure 3 Tensile yield strength versus glass bead content at several crosshead displacement rates. ■ 2, ○ 5, ⊕ 10, □ 20, ⊞ 50, △ 200 mm min^{-1}.

tensile yield strength of the ASA polymer decreases as more and more glass beads are added. Results indicate, that tensile yield strength decreases linearly as the volume fraction of the glass beads is increased, regardless of the testing rate. This behaviour is consistent with the predictions for particulate filled systems, as presented by Piggott and Leinder [1]

$$\sigma_c = \lambda\sigma_m - \varkappa\phi_f \quad (2)$$

where λ is the stress concentration factor and $\varkappa$ is a constant dependent upon the filler-polymer adhesion. As shown in Table II, values of λ and $\varkappa$ are not significantly affected by the rate of testing; values of λ range from 0.99–0.97 and those of $\varkappa$ range from 94–105. Data in Fig. 3 is replotted in Fig. 4 as relative strength (tensile yield strength of the filled polymer divided by the tensile yield strength of the unfilled polymer) versus glass bead content. Fig. 4 shows that relative strength is more or less independent of the loading rate. It is worth noting that the introduction of 18% by volume glass beads into ASA polymer resulted in a reduction in tensile yield strength value by about 40%. This reduction in tensile strength with increasing ϕ_f suggests that the presence of glass beads has a weakening effect rather than a strengthening one. As in other glass bead filled systems [e.g. 2–7], upon loading, glass beads tend to debond from the matrix and as a results of this, the volume fraction of composite carrying the load falls, the matrix becomes full of holes analogous to that of Swiss cheese, and the large-scale plastic deformation is reduced.

The effect of crosshead displacement rate $x°$, on tensile yield strength is depicted in Fig. 5, where it can be seen that tensile yield strength for ASA and its composites increases linearly with log $x°$, i.e.

$$\sigma_c = K_1 + K_2 \log x° \quad (3)$$

Values of constants K_1 and K_2 are delineated in Table III. Analogy with the Eyring model [8] for yielding suggests that from constant K_2 one may estimate the activation volume, v^*, of the material. These values are also given in Table III and it can be seen the introduction of glass beads into ASA polymer

TABLE II Rate effect

$x°$	λ (MPa)	$\varkappa$
2	0.99	94.4
5	0.99	98.3
10	0.99	100.1
20	0.99	103.0
50	0.98	105.4
100	0.97	105.4

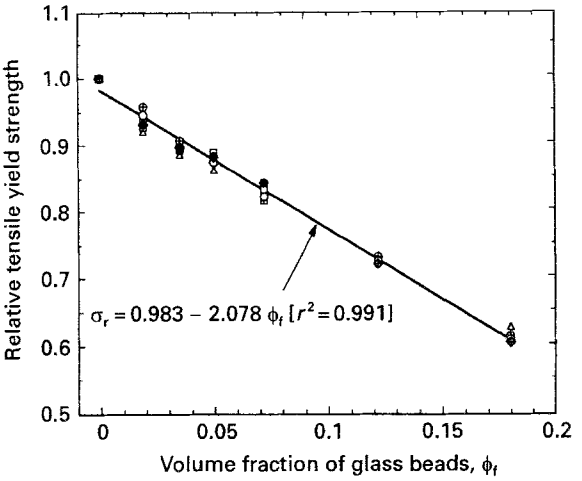

Figure 4 Relative tensile yield strength versus glass bead content at several crosshead displacement rates. ⊕ 2, ○ 5, ⊕ 10, □ 20, ⊞ 50, △ 200 mm min^{-1}.

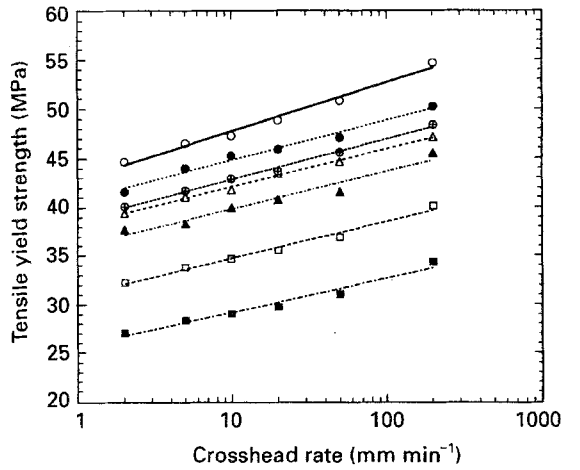

Figure 5 Tensile yield strength versus log(loading rate) for various glass bead contents. ϕ_f = ○ 0, 0.019 ●, 0.035 ⊕, 0.05 △, 0.072 ▲, 0.122 □, 0.18 ■.

TABLE III Rate effect

ϕ_f	K_1	K_2 ($\times 10^6$)	v^*(m^3 mol^{-1})($\times 10^{-3}$)
0	42.74	4.952	2.32
0.020	40.69	4.062	2.83
0.035	38.65	4.121	2.79
0.050	38.14	3.872	2.97
0.072	35.92	3.829	3.00
0.122	30.88	3.792	3.03
0.180	25.65	3.485	3.30

increases v^* thus indicating that the ability of the material to yield is hindered due to presence of the glass beads of the material.

The influence of ϕ_f on tensile strength at break, σ_b, is shown in Fig. 6 as the ratio σ_b/σ_y for several crosshead speeds. As can be seen, variation can be described by two straight lines with a transition occurring at a ϕ_f value of about 3.5%. Below this value, strength ratio seems to be very sensitive to small changes in ϕ_f whereas above this value the ratio changes at much slower rate with respect to ϕ_f. Extrapolation to $\sigma_b/\sigma_y = 1$ suggests that brittle failure occurs when glass bead content exceeds 23%. It is noteworthy that the ratio σ_b/σ_y is not affected significantly by the rate of testing.

The influence of ϕ_f on work of fracture is shown in Fig. 7. The general trend is that work of fracture decreases with increasing ϕ_f. This reduction is caused by the reduction in the overall resin strain and strength with increasing ϕ_f. It is worth mentioning that values of work of fracture exhibited high degree of scatter which prevented us from drawing any conclusion with respect to loading rate.

The effect on weldline on tensile behaviour is illustrated in Fig. 8, where it can be seen that the presence of the weldline promotes brittle failure in ASA polymer and all its composites. The influence of weldline on tensile strength as a function of glass bead content is shown in Fig. 9(a) and (b) for crosshead displacement rates of 5 and 50 mm min^{-1}. Evidently, for the range of ϕ_f values tested, weldline strength is also a linear function of ϕ_f and, for constant volume fraction of glass bead, its value is lower than tensile yield strength of the weld free specimen. The weldline integrity factor, F, which is often defined as the strength of the specimen with a weldline divided by the strength of the weld-free specimen fell within the range 0.83–0.92 as illustrated in Fig. 10. Although the difference between the lowest and the highest weldline factor is only 10% for the range of ϕ_f values tested, and therefore not very significant, nevertheless it seems that tensile yield strength is less affected by the weldline when glass bead concentration is high. Thus suggesting that as ϕ_f increases, the weakening of the material due to the presence of the weldline is masked by that caused due to the presence of the glass beads in the material. It is worth noting that the extent of weldline induced mechanical weakness does not appear to be dependent on the loading rate, at least within the range employed here.

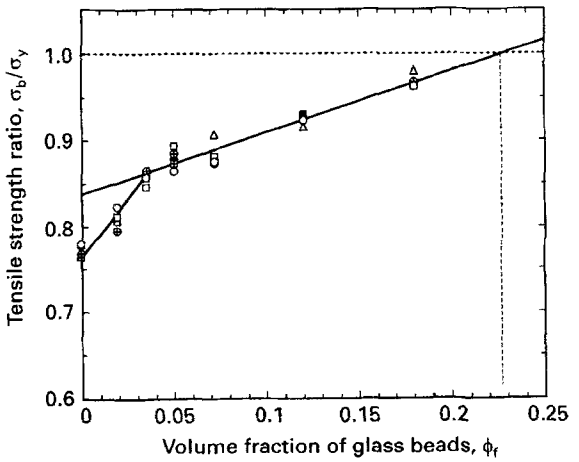

Figure 6 The effect of glass bead content on tensile strength ratio at several crosshead displacement rates. ○ 5, ⊕ 10, □ 20, ⊞ 50, △ 200 mm min^{-1}.

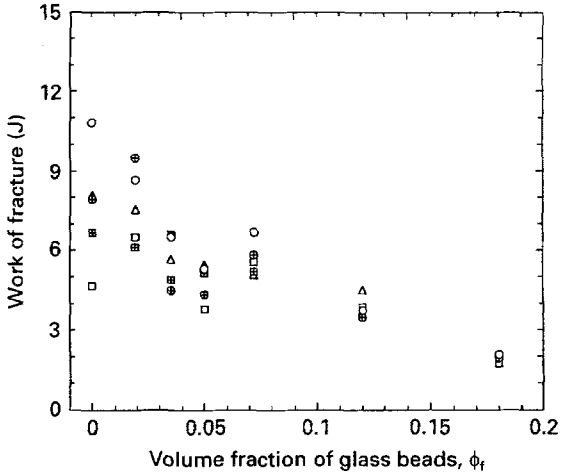

Figure 7 Work of fracture versus volume fraction of glass beads at several crosshead displacement rates. ○ 5, ⊕ 10, □ 20, ⊞ 50, △ 200 mm min^{-1}.

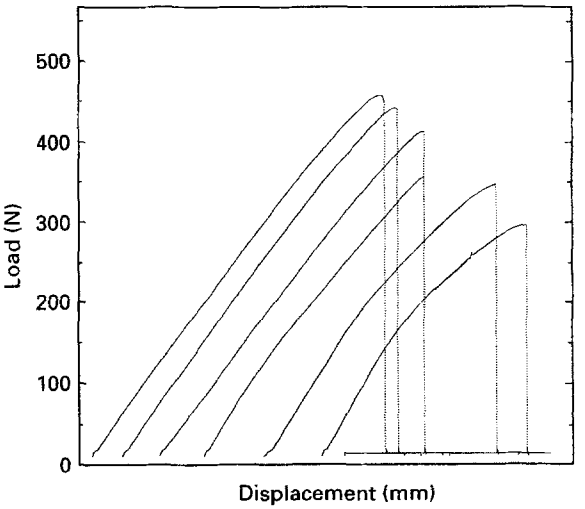

Figure 8 Typical tensile load–displacement diagrams for ASA polymer and its composites with a weldline at loading rate of 5 mm min^{-1} (From left to right for: 0%, 2%, 5%, 7.2%, 12.2% and 18% by volume glass beads.)

4.2. Flexural tests

Three point bend flexural modulus and strength as a function of glass bead content were determined by testing flexure bars of dimensions 120 × 10 × 4 mm at a crosshead displacement rate of 5 mm min^{-1} with span width of 64 mm. Flexural load–displacement traces for ASA and its composites showed a clear maximum load. None of the specimens fractured under this mode. Modulus and strength for each material were computed from the initial slope and maximum load

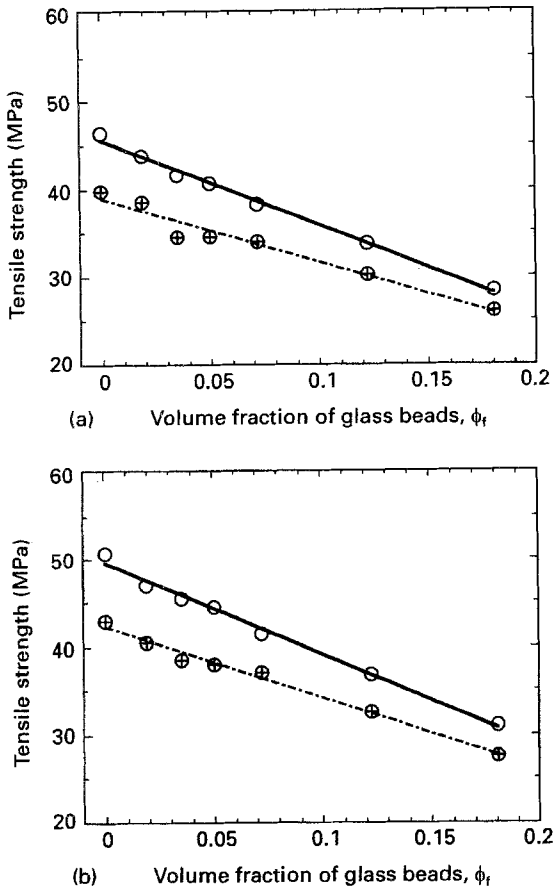

Figure 9 The comparison between the tensile yield strengths of the specimens with (⊕) and without (○) weldlines: (a) 5 mm min^{-1} and (b) 50 mm min^{-1}.

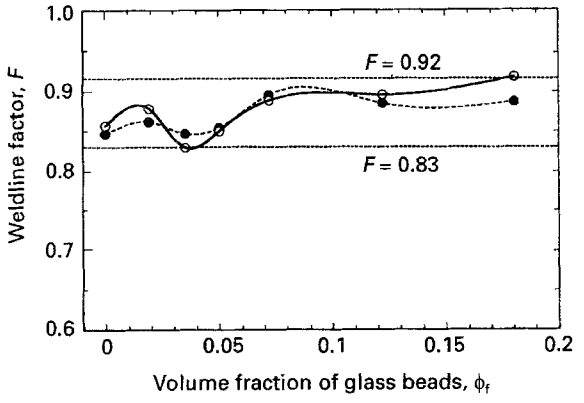

Figure 10 Weldline factor, F, versus glass bead content. ○ 5, ● 50 mm min^{-1}.

on the trace respectively, using the following equations

$$E_f = \frac{1}{4B}\left(\frac{P}{\delta}\right)\left(\frac{S}{D}\right)^3$$

$$\sigma_f = \frac{3p_m S}{2BD^2} \quad (4)$$

where (P/δ) is the initial slope of the load–displacement diagram, p_m is the maximum load, B and D are the specimen thickness and depth, repectively, and S is the span width.

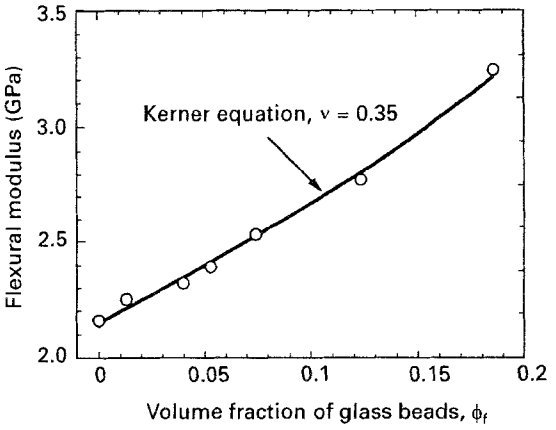

Figure 11 Flexural modulus versus glass bead content.

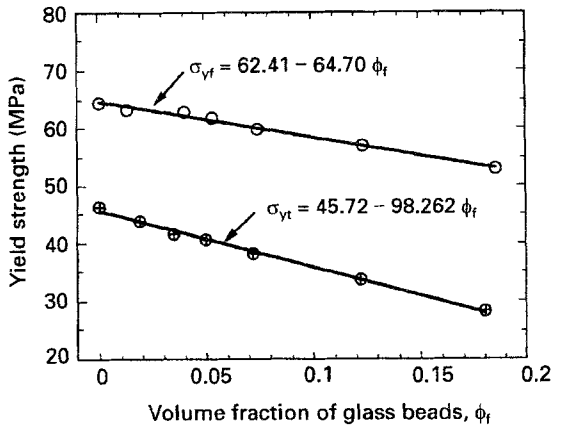

Figure 12 Flexural yield strength versus glass bead content. ○ Flexure, ⊕ tensile.

Fig. 11 shows the dependence of the initial modulus on the volume fraction of glass beads. As expected, a significant increase in modulus is obtained as glass bead concentration is increased. This increase in initial modulus with glass bead concentration follows Kerner's equation [9]

$$E_c = E_m\left(1 + \frac{15\phi_f(1 - \nu_m)}{(1 - \phi_m)(8 - 10\nu_m)}\right) \quad (5)$$

for moduli up to the volume fractions investigated. ($\nu_m = 0.35$).

The dependence of the flexural strength on volume fraction of glass beads is shown in Fig. 12 and compared with that obtained from tensile tests. Although the dependence is linear and therefore follows the same pattern as that observed for tensile yield strengths, comparison shows that flexural yield strength is always higher than tensile yield strength and the value of χ in bending is lower than those obtained from the tensile experiments. The ratio of the flexural yield strength divided by tensile yield strength increased from 1.38 to 1.87 as volume fraction of glass beads was increased from 0 and 18.5%. It is worth noting that in tensile tests, when particles separate from the matrix, the load thereafter is carried by the polymer matrix. Fracture therefore takes place when the matrix surrounding the vacuoles is under

a stress which is equal to the ultimate tensile strength of pure resin. In bending however, failure takes place by a crack propagating from the tension side to the compression side of the beam. The presence of the beads hinders crack propagation and this could lead to higher strengths in flexural specimens than that of tensile specimens. Obviously, crack propagation becomes more difficult as ϕ_f is increased, leading to a greater difference between tensile and flexural strengths as observed here. The volume of the material under the test and the skin-core morphology were also thought to be contributing factors, even though their effect was not investigated here.

4.3. Impact energy

Notched and unnotched impact energies as a function of glass bead content were measured using three-point Charpy impact specimens of thickness, B, and depth, D, of 4 and 10 mm respectively. Specimens were fractured at the pendulum speed of 3 m s^{-1} and span width of 40 mm. Notched impact tests were performed with a/D ratio of 0.3 using a V-shaped cutter with a tip radius of 0.25 mm. The effect of glass bead content on impact energy per unit area of the uncracked section (i.e. U/BD for unnotched and U/BL for notched where $L = D - a$) is shown in Fig. 13(a), where each datum represents the average of five to twenty measurements. As can be seen, a clear drop in impact energy is observed for both notched and unnotched specimens, as glass bead content is increased (the unnotched impact energy for the unfilled ASA was 113 kJ m^{-2}). However the data suggest that impact energy per unit area for notched specimens is less influenced by the glass bead content than those of unnotched specimens. If we define a notch integrity factor, F_N, as U/BL, divided by U/BD then as shown in Fig. 13(b) we observe that F_N increases as more and more glass beads are added to the polymer. Clearly, the polymer matrix is very notch sensitive as indicated by a low F_N value of 0.12. However, notch effect becomes increasingly less sensitive as more and more glass beads are added. Indeed, as shown in Fig. 13(b), adding 1.3% by volume of beads increases F_N by a factor of 3. It is worth noting that the notch effect becomes completely masked by the glass beads when bead concentration reaches 18% by volume and F_N becomes unity.

4.4. Fracture tests

Fracture tests were performed on single-edge notched bend specimens (SENB) of dimensions $B = 4$ mm, $D = 10$ mm and length of 100 mm as shown in Fig. 13(a). For each material, a series of SENB specimens were prepared with the notch depth a, ranging from 2 to 7 mm. All the specimens were razor notched and tested in three-point bending configuration at crosshead displacement rates of 5, 50 and 500 mm min^{-1} with span to depth ratio (S/D) being fixed at 4:1. The load–displacement trace for each material was recorded for subsequent analysis.

Fig. 14(a–c) show typical SENB load curves obtained in this study. As can be seen, all the curves

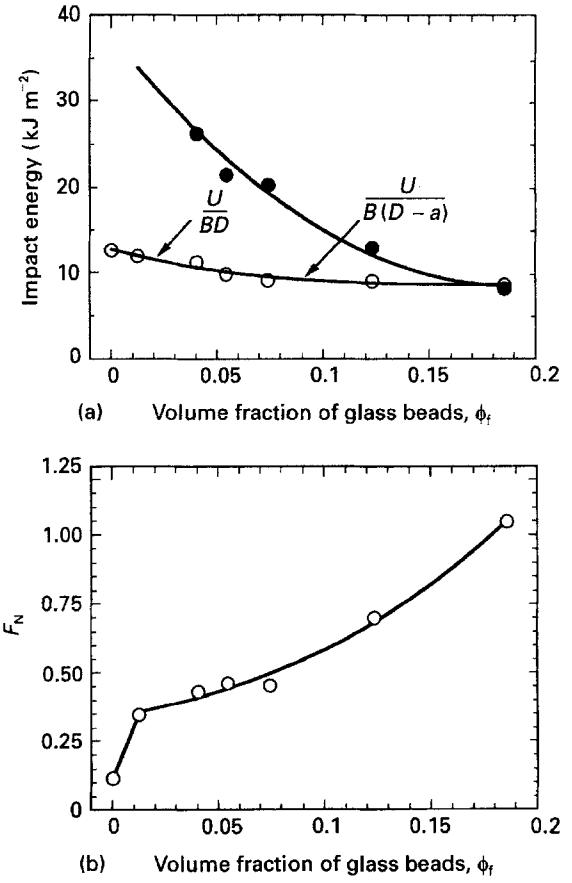

Figure 13 (a) Impact energy per unit area for notched and unnotched specimens as a function of glass bead content. (b) Notch integrity factor versus glass bead content.

indicate slow crack propagation up to the complete failure of the test specimen.

To determine the resistance of the unfilled and filled ASA materials to crack propagation as a function of glass bead content and testing rate, the generalized locus method developed by Kim and Joe [10] was employed. This method has been used successfully to study the effect of compatibilizer on the mechanical properties of nylon 6 and ABS polymer blend [11, 12].

The Kim and Joe approach, which in effect is an extension of the J-integral, seeks to determine the resistance of the material to crack initiation in terms of the critical J-integral value, J_c, and the resistance of the material to crack propagation in terms of J_R, by utilizing the locus line of crack initiation points or failure points on load–displacement records.

The energy rate interpretation of the J-integral as proposed by Rice [13] states that;

$$J = -\frac{1}{B}\frac{dU}{da}\bigg|_{\text{constant displacement}} \tag{6}$$

where B is the specimen thickness and a is the crack-length. However, if it is assumed that J has a constant value, J_c, at crack initiation points, and a constant value, J_R, at failure points, then Equation 6 can be generalized to give

$$J_c = -\frac{1}{B}\frac{\Delta U_c}{\Delta a} \tag{7}$$

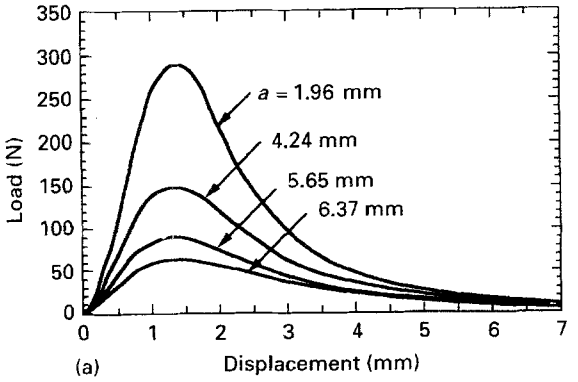

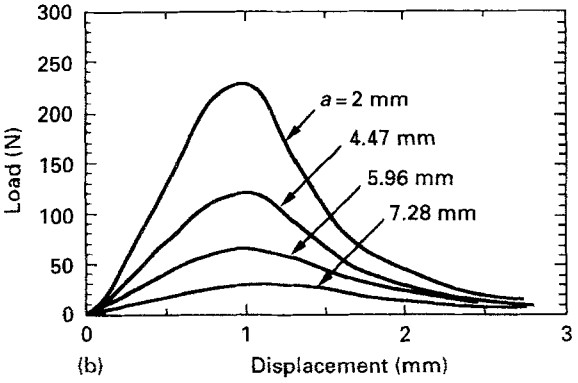

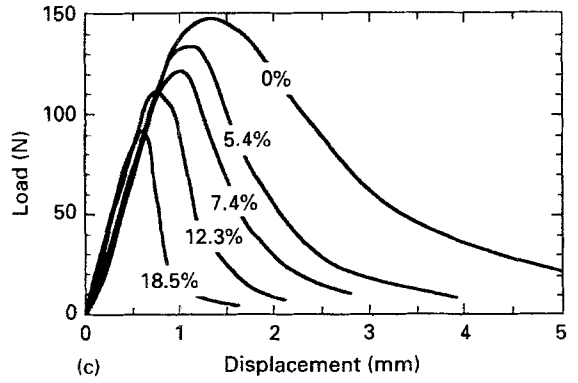

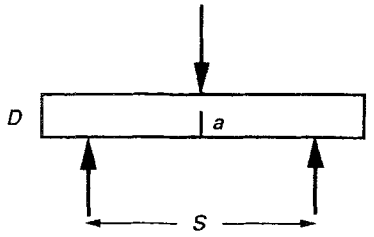

Figure 14 Typical SENB load-displacement diagrams. (a) ASA polymer tested at 5 mm min^{-1} for a range of crack length values. (b) ASA polymer filled with 12.3% by volume glass beads tested at 5 mm min^{-1} for a range of crack length values. (c) ASA polymer and few selected composites tested at 5 mm min^{-1} and fixed crack length.

for crack initiation where U_c can be determined from the area bounded by the loading curve, the locus line of crack initiation points, and the x-axis and

$$J_R = -\frac{1}{B}\frac{\Delta U_T}{\Delta a} \quad (8)$$

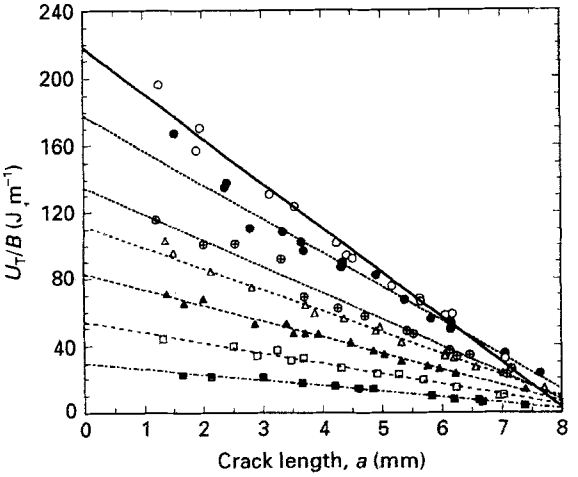

Figure 15 Total work of fracture per unit thickness versus crack length for ASA polymer and its composites at a constant crosshead displacement rate of 5 mm min^{-1}. ○ 0, ● 1.3, ⊕ 4, △ 5.4, ▲ 7.4, □ 12.3, ■ 18.5 %.

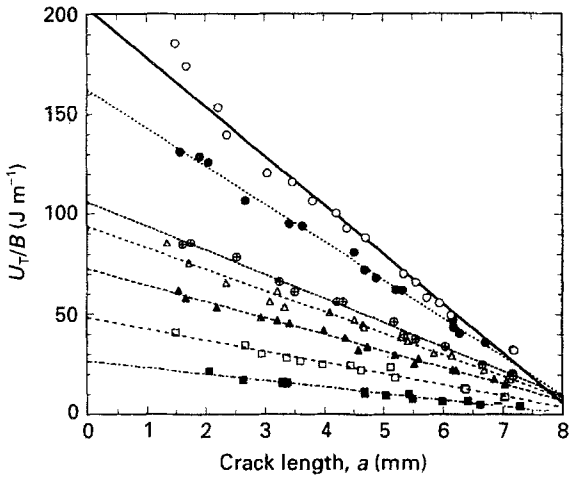

Figure 16 Total work of fracture per unit thickness versus crack length for ASA polymer and its composites at a constant crosshead displacement rate of 50 mm min^{-1}. ○ 0, ● 1.3, ⊕ 4, △ 5.4, ▲ 7.4, □ 12.3, ■ 18.5%.

for crack propagation where in this case U_T represents the total energy for fracture (total area enclosed by the curve and the x-axis).

Based on Equations 7 and 8 J_c may then be found by plotting U_c per unit thickness (U_c/B) versus a and J_R may be found by plotting U_T per unit thickness (U_T/B) versus a. If these plots are linear then J_c and J_R are constants and their values can be determined from the slopes of the lines.

Following the procedure outlined above, the total energy for fracture, U_T, for each specimen was measured from the area under the load–displacement diagrams and plotted in accordance with Equation 8. These plots are shown in Figs 15 to 17 for loading rates of 5, 50 and 500 mm min^{-1} respectively. As can be seen, variations of U_T/B with respect to crack length are fairly linear particularly for crack lengths greater than 2 mm. The slope of the least square linear fitted line through each set of data was taken as an average resistance to steady crack propagation, J_R. These values are plotted in Fig. 18 as a function of

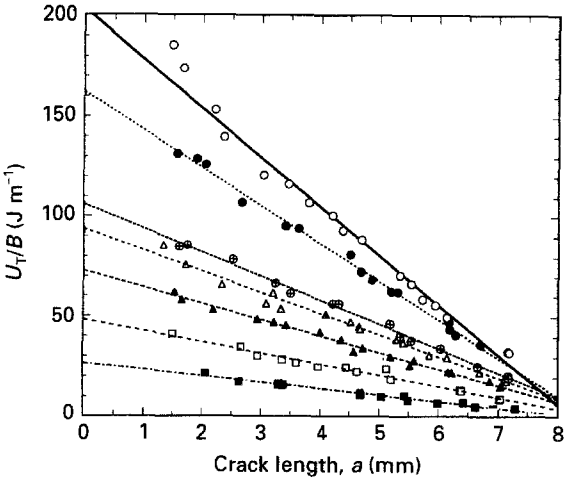

Figure 17 Total work of fracture per unit thickness versus crack length for ASA polymer and its composites at a constant crosshead displacement rate of 500 mm min^{-1}. ○ 0, ● 1.3, ⊕ 4, △ 5.4, ▲ 7.4, □ 12.3, ■ 18.5 %.

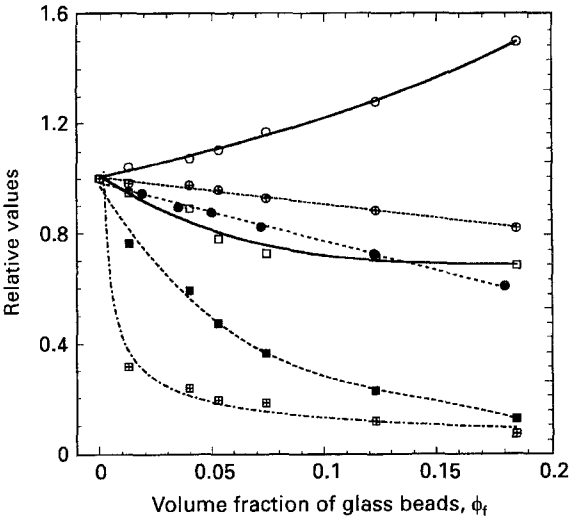

Figure 20 Relative values versus glass bead content. ⊕ Flexural yield strength; ○ flexural modulus; ● tensile yield strength; □ impact/notched; ⊞ impact/unnotched; ■ Gp.

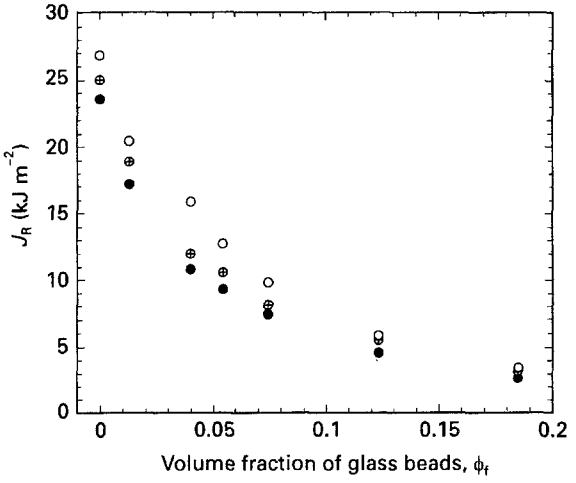

Figure 18 J_R versus glass bead content for ASA polymer and its composites. ○ 5, ⊕ 50, ● 500 mm min^{-1}.

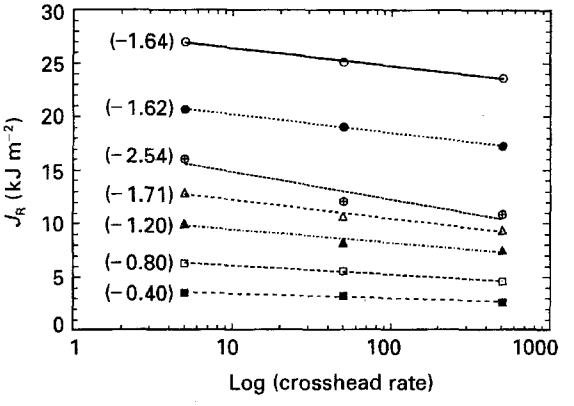

Figure 19 J_R versus crosshead displacement rate for ASA polymer and its composites. ○ 0, ● 1.3, ⊕ 4, △ 5.43, ▲ 7.43, □ 1.3, ■ 18.5%.

glass bead content, ϕ_f for the three loading rates used. It can be seen that the addition of glass beads to the polymer decreases the resistance of the material to steady crack propagation. This reduction in J_R with glass bead content is caused by inhibition of the plastic flow near the glass bead surfaces where there is little possibility of stress transfer from the polymer to the beads. It is worth noting for the range of ϕ_f values tested, the variation of J_R with loading rate is fairly linear as shown in Fig. 19. From the slopes of these lines (values given inside the parentheses in Fig. 19), one may conclude that the rate at which J_R changes with loading rate is affected by the amount of glass bead present in the material. Apart from the composite with glass bead content of 4% which surprisingly shows the highest slope, the trend appears to be a reduction in slope with increasing ϕ_f particularly when ϕ_f exceeds 5.43%.

5. Summary

It was the objective of this work to investigate the influence of glass bead content on the mechanical properties of ASA copolymer. Properties such as tensile and flexural yield strength, work of fracture, flexural modulus, impact energy were all found to be strongly influenced by the addition of glass beads to ASA. Tensile and flexural yield strengths were linearly decreasing functions of glass bead content in accordance with Leinder's equation. The total work of fracture and impact energy of the notched and unnotched specimens all decreased with increasing glass bead content. The only improvement in the material performance was that of flexural modulus which showed an increase with increasing glass bead content, in accordance with Kerner's equation. Addition of the glass beads also had a dramatic effect on the resistance of the material to steady crack propagation. This resistance to crack propagation was found to be a linear and decreasing function of loading rate.

Fig. 20 summarises the relative values of some of the quantities that were measured in this study. Clearly, introduction of the glass beads into the polymer affects some quantities more drastically than others. As can be seen, fracture related parameters such as J_R or impact energy are more affected by the bead concentration than the tensile or flexural yield strengths.

Acknowledgement

The authors gratefully acknowledge the support provided by BASF in providing the materials.

References

1. M. R. PIGGOT and J. LEINDER, *J. Appl. Polym. Sci.* **18** (1974) 1619.
2. N. J. MILLS, *ibid* **15** (1971) 2791.
3. D. L. FAULKNER and L. R. SCHMIDT, *Polym. Engng. Sci.* **17** (1977) 657.
4. K. L. TRACHTE and A. T. DIBENEDETTO, *Int. J. Polym.* **1** (1971) 75.
5. H. ZHANG and L. A. BERGLUND, *Polym. Engng. Sci.* **33** (1993) 100.
6. L. NICOLAIS, E. DRIOLI and R. F. LANDEL, *Polymer* **14** (1973) 21.
7. S. HASHEMI, K. J. DIN and P. LOW, in press.
8. N. G. McCRUM, C. P. BUCKLEY and C. B. BUCKNALL, "Principles of polymer engineering" (Oxford Science Publications, Oxford, 1989).
9. S. AHMED and F. R. JONES, *J. Mater. Sci.* **25** (1990) 4933.
10. B. H. KIM and C. R. JOE, *Polymer Testing* **7** (1987) 355.
11. D. M. OTTERSON, B. H. KIM and R. E. LAVENGOOD, *J. Mater. Sci.* **26** (1991) 1478.
12. *Idem., ibid.* **26** (1991) 4855.

Received 2 October
and accepted 9 November 1995